

Biermann, L.: The connection between active regions on the sun and coronal condensations was discussed in some detail at the I. A. U. symposium on the solar corona in Cloudcroft, N.M., last week. The evidence is that this connection is quite a regular one, hence the fact, that the densities derived from the type III bursts are regularly considerably higher than those derived from any of the standard models of the corona, is easily understood.

JOURNAL OF THE PHYSICAL SOCIETY OF JAPAN Vol. 17, SUPPLEMENT A-II, 1962
INTERNATIONAL CONFERENCE ON COSMIC RAYS AND THE EARTH STORM Part II

II-3A-8. The Sizes of the Sources of Solar Radio Bursts at 40 and 60 Mc/s*

A. A. WEISS and K. V. SHERIDAN

C.S.I.R.O. Radiophysics Laboratory, Sydney, Australia

§1. Introduction

A swept-phase interferometer has been used in conjunction with the Depto radio spectrograph and the swept-frequency interferometer to study the angular sizes of the sources of the bursts of radio emission from the Sun. Measurements are made at either 40 or 60 Mc/s, at the discretion of the operator, and with aerial spacings $a=1$ km (long base) or $a=\frac{1}{4}$ km (short base).

The parameter measured is the visibility, ξ , of the fringes, defined by $\xi=(P_{\max.}-P_{\min.})/(P_{\max.}+P_{\min.})$. $P_{\max.}$ and $P_{\min.}$ are the maximum and minimum envelopes of the interference pattern of the source. If the relative attenuation of the feeder lines of the two aerials is α nepers, $\xi \cosh \alpha$ is the ratio of the moduli of the Fourier components of the source distribution at angular "frequencies" $(\alpha/\lambda) \cos \theta_0$ and 0 (Wild and Sheridan 1958). The effect of foreshortening ($\theta_0 \neq 0$) is neglected here.

The observational material discussed in this paper consists almost entirely of pairs of visibility measurements ($\xi_s \cosh \alpha$, $\xi_L \cosh \alpha$) made with the two aerial spacings within half a second of each other. A full assessment of all the available data has yet to be made, and this report is preliminary in nature.

§2. Bursts of Types II and IV

Visibilities for eight Type II bursts, and for the Type IV continuum following the 3⁺ flare of 15 November 1960, are plotted in Fig. 1. The Type IV measurements were averaged over a 45 min. period, during which the source position remained essentially fixed; this period commenced about 30 min. after the start of the flare. If this latter event is typical of Type IV, the location of the points in the ξ_s - ξ_L plane suggests that sources of Type II and Type IV emission are characterized by differently-shaped bright-

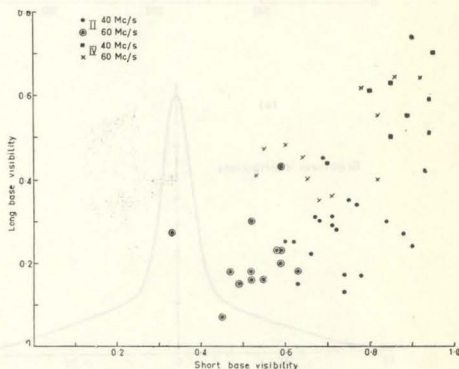


Fig. 1. Plot of long base vs. short base visibilities for eight Type II bursts and the Type IV continuum of 15 November 1960. Visibilities have been corrected for attenuation in the aerial feed lines.

* This paper was read by J. P. Wild.

ness distributions. No significant differences were found between visibilities for fundamental and harmonic bands of Type II bursts, and they have not been differentiated in Fig. 1.

Long and short base positions of sources of Type II bursts measured with the swept-frequency interferometer often disagree. This suggests that the brightness distributions are complex and asymmetrical. However, the discrepancy in position is usually a good deal less than half the long base lobe separation, and in all but 2 out of 31 cases, $\xi_s > 2\xi_L$. It is therefore improbable that Type II sources have more than one pronounced maximum.

Observations of the visibility at only two aerial spacings are inadequate for the determination of the brightness distribution, but it seems reasonably certain that the observations cannot be interpreted in terms of any simple single-humped brightness distribution. For Type II bursts and assuming symmetrical sources, we find that the measurements are consistent with the brightness distribution at 40 Mc/s being the same as at 60 Mc/s. This allows us to combine the

observations at the two frequencies, so obtaining five points on the transform (Fig. 2 (a)). With this assumption the visibility measurements have been fitted by the sum of two Gaussian curves. The resulting brightness distribution consists of a central condensation ("core") superimposed on a diffuse background ("halo") (Fig. 2(a)).

More extensive long base visibility measurements, interpreted according to this model, indicate that, apart from minor fluctuations, the size of each Type II source is almost constant over the lifetime of the burst, with a suggestion that the size increases towards the end of the burst. Source sizes for different Type II events (both fundamental and harmonic bands) are similar, and appear to be independent of spectral characteristics (bandwidth, multiple structure) and of position on the solar disc.

For the Type IV continuum of 15 November 1960, long and short base positions differed by some 5', suggesting a slight asymmetry in the source. Such asymmetry may not be typical of this class of event, for which the two sets of position measure-

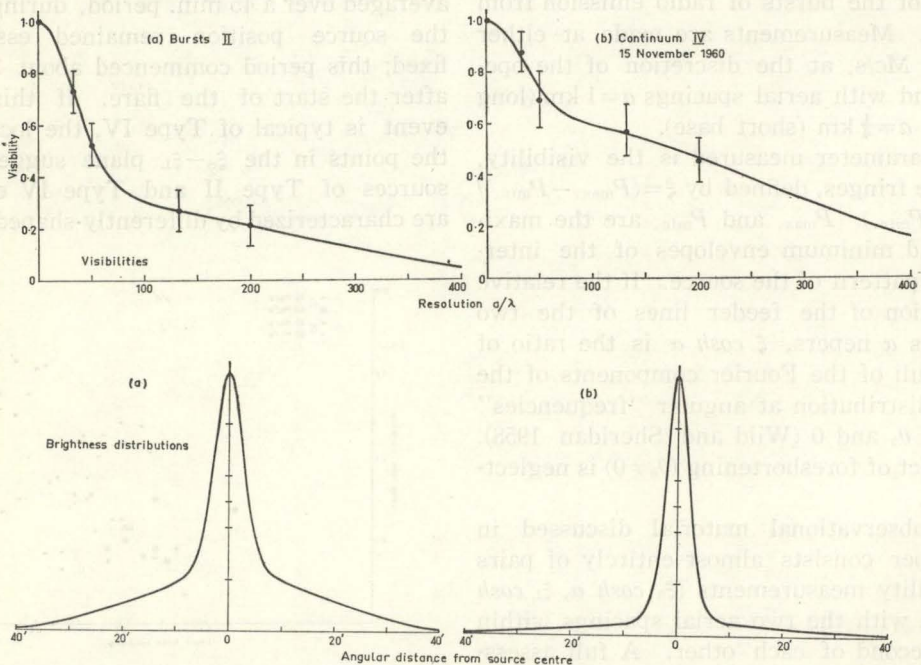


Fig. 2. Observed visibilities and brightness distributions derived from them on the assumption that the source structure is the same at 40 and 60 Mc/s.

(a) average of eight Type II bursts

(b) Type IV continuum of 15 November 1960.

ments often agree within the observational errors. Retaining, here with more justification, the assumptions of a symmetrical source and a brightness distribution independent of frequency (in our range), we find (Fig. 2(b)) that the strength of the halo for the Type IV source is much less than for the Type II sources. If we do not make the assumption that the brightness distribution is the same at 40 and at 60 Mc/s, there are only three points for each transform, and these cannot be fitted uniquely by the sum of two Gaussian curves. However, the width of the core and the relative contribution of the halo to the total power do not depend strongly on the width of the halo provided the latter is not too small, and some information about the brightness distributions can be obtained by assuming a reasonable width for the halo.

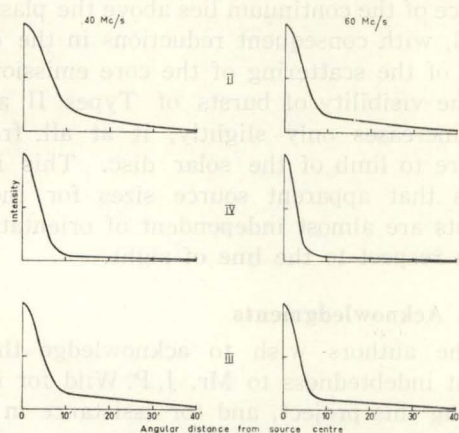


Fig. 3. Brightness distributions computed on the assumption of a halo width of $40'$ to $\exp(-\frac{1}{2})$ power points.

Fig. 3 shows the brightness distributions for Type II and IV bursts for a halo width of $40'$ between $\exp(-\frac{1}{2})$ power points. This assumption leads to core widths which are larger at 40 Mc/s than at 60 Mc/s, but once again we see that the strength of the halo for the Type IV source is much less than for the Type II sources.

§ 3. Bursts of Type III

The brightness distribution for simple Type III bursts changes progressively during the lifetime of the burst. This development is illustrated in Fig. 4 for 12 simple Type III bursts at 40 Mc/s. Each of these bursts

showed an exponential rise and decay of intensity, and the individual intensity measurements are plotted in Fig. 4(c). The mean visibility curves (Fig. 4(b)), from which the brightness distributions of Fig. 4(a) were computed assuming an infinite halo, are averages for the 12 bursts, and it is possible that the initial size of the core for most bursts is no larger than at maximum intensity. There is no doubt, however, that the post-maximum increases in apparent angular size of the core, and of the relative intensity of the halo, are real.

Visibility data for Type III bursts whose spectra are more complex than those of the simple Type III bursts already considered are also available. A detailed examination of this material suggests that the brightness distributions at 40 and at 60 Mc/s are not identical, and mean brightness distributions have therefore been computed, as was done for events of Types II and IV, by assuming a halo width of $40'$ between $\exp(-\frac{1}{2})$ power points. These brightness distributions, which

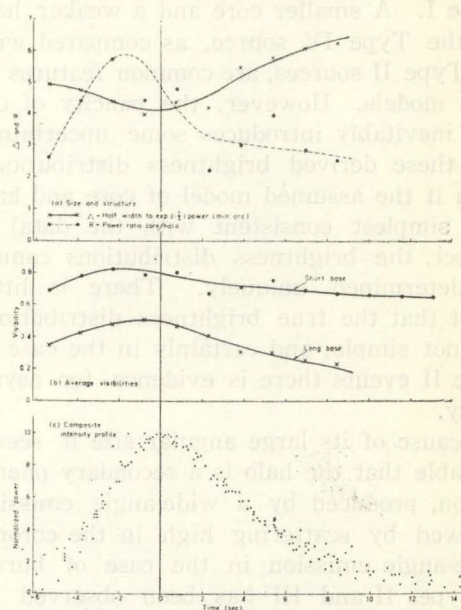


Fig. 4. The temporal variation of 12 simple Type III bursts, 40 Mc/s. All events have been reduced to standard duration.

- (a) core width and power ratio core/halo, assuming a halo of infinite width.
- (b) average visibilities, corrected for feeder attenuation.
- (c) normalized intensity variations; points are from individual bursts.

Table I. Characteristics of Brightness Distributions

Type of Burst	No. of Events	Model A*			Model B**				Remarks
		Power Ratio Core/Halo	Core Half Width***	Halo Half Width***	40 Mc/s		60 Mc/s		
					Power Ratio Core/Halo	Core Half Width***	Power Ratio Core/Halo	Core Half Width***	
II	8	0.5	3.1'	20'	1.1	5.5'	0.8	4.0'	{Change over lifetime of burst
III	44	—	—	—	0.9	4.1'	1.4	3.4'	
IV	1	2.1	2.7'	20'	4.1	4.0'	1.8	2.7'	

* Assumes brightness distribution independent of frequency.
** Assumes halo width of 48' between half-power points.
*** Half width to half-power points.

are illustrated in Fig. 3, have core widths larger at 40 than at 60 Mc/s, and halos comparable in strength with those of Type II sources.

§ 4. Discussion

Some characteristics of the brightness distributions obtained with the two models considered in this paper are summarized in Table I. A smaller core and a weaker halo for the Type IV source, as compared with the Type II sources, are common features of both models. However, the paucity of the data inevitably introduces some uncertainty into these derived brightness distributions. Even if the assumed model of core and halo (the simplest consistent with the data) is correct, the brightness distributions cannot be determined uniquely. There is little doubt that the true brightness distributions are not simple, and certainly in the case of Type II events there is evidence for asymmetry.

Because of its large angular size it seems probable that the halo is a secondary phenomenon, produced by a wide-angle emission followed by scattering high in the corona. Wide-angle emission in the case of bursts of Types II and III has been observed by Roberts (1959) and by Wild, Sheridan and Neylan (1959), who suggested as the cause scattering on small scale irregularities near the plasma level. However, generation of the bursts in dense coronal streamers might

well produce a similar result. The weaker halo of the Type IV continuum, as compared with the halo for the Type II burst which preceded it, is easily understandable if the source of the continuum lies above the plasma level, with consequent reductions in the extent of the scattering of the core emission.

The visibility of bursts of Types II and III increases only slightly, if at all, from centre to limb of the solar disc. This implies that apparent source sizes for these bursts are almost independent of orientation with respect to the line of sight.

§ 5. Acknowledgments

The authors wish to acknowledge their great indebtedness to Mr. J. P. Wild for initiating this project, and for assistance in its development and in interpretation of results. They also wish to thank Dr. J. A. Roberts for valuable discussion and criticism, Mr. G. H. Trent and Mr. J. Joisce for assistance with observations, Mr. K. R. McAlister for assistance in design of equipment, and Miss Julie Todd for painstaking reduction of records.

References

J. A. Roberts: *Aust. J. Phys.* **12** (1959) 327.
J. P. Wild: *Aust. J. Sci. Res. A.* **3** (1950) 541.
J. P. Wild and K. V. Sheridan: *Proc. I.R.E.* **46** (1958) 160.
J. P. Wild, K. V. Sheridan and A. A. Neylan: *Aust. J. Phys.* **12** (1959) 369.

Discussion

Takakura, T.: You did not mention about a difference of heights between the

fundamental and the second harmonic of type III and II bursts. We would like to hear the difference.

Wild, J. P.: Recent work by Smerd, Sheridan and me (presented at the I. A. U. meeting at Berkeley) has shown that in 4 out of 4 cases the second harmonic of a type II burst arrives from a position considerably *closer* to the solar flare than the fundamental observed (minutes before) at the same frequency. The simple application of the plasma hypothesis would suggest just the opposite. However, if it is supposed that the outward moving stream excites harmonic radiation dominantly in the *inward* direction, then the result can be explained using the conventional ray trajectories of the reflected ray. We have formed that such inward propagation appears to be consistent with the theory of Ginzburg and Zherezniakov that the harmonic radiation originates from combination scattering of a Cerenkov plasma wave in the thermal corona.

Corresponding measurements for type III bursts are inconclusive.

Morimoto, M.: We have many examples of a very much extended source of type II burst at 200 Mc/s. Is there any phase inversion in the fringe of the wider separation antenna system?

Wild: The phase of the pattern recorded with the wide space interferometer relative to the narrow space can vary considerably, especially in the case of type II bursts for which complete phase reversal can sometimes occur. The assumption of symmetry therefore involves a very coarse approximation with these bursts.

JOURNAL OF THE PHYSICAL SOCIETY OF JAPAN Vol. 17, SUPPLEMENT A-II, 1962
INTERNATIONAL CONFERENCE ON COSMIC RAYS AND THE EARTH STORM Part II

II-3A-9. A Model of the Coronal Condensation

Eijiro HIEI

Tokyo Astronomical Observatory, Tokyo, Japan

The electron density and the electron temperature of the coronal condensation were determined by the optical observation at the total solar eclipse of October 12, 1958 in the South Pacific. The distribution of the electron density was derived from the direct photographs of the corona. At 100,000 km above the photosphere the electron density was ten times higher in the condensation than in the normal corona. The temperature is uncertain owing to the ambiguity in collisional cross-section. From the equivalent widths of three emission lines, *i.e.*, $\lambda\lambda$ 3987 Fe XI, 4086 Ca XIII and 4231 Ni XII appearing on our flash spectrograms, the electron temperature was estimated to be slightly higher in the condensation than in the normal corona.

§ 1. Introduction

Many studies on the coronal condensation have so far been made by radio techniques¹⁾. From optical observations we have as yet little information as to the model of the condensation because of the difficulty of observation. The intensity of the coronal condensation is optically faint and severely affected

by the strong intensity of the photosphere. With a coronagraph we may be able to observe emission lines²⁾⁻⁴⁾ of the condensation. The results are mainly used to deduce the temperature. However, the intensity of the continuum^{2), 3)} of the condensation, which will give the electron density, is difficult to observe. With a *K*-coronameter we could observe